Solvation Free Energies of the Fullerenes C_{60} and C_{70} in the Framework of Polarizable Continuum Model

Evgeny B. Stukalin, Mikhail V. Korobov,* and Natalia V. Avramenko

Department of Chemistry, Moscow State University, Moscow 119992, Russia

Received: March 5, 2003; In Final Form: May 23, 2003

In the present study the scaled particle theory (SPT) along with the polarizable continuum model (PCM) were used to describe the thermodynamics of solvation of the fullerenes C_{60} and C_{70} in aromatic solvents, hexane, and water. The various contributions to the solute−solvent interaction were calculated within PCM based on effective Hamiltonians. The cavitation energy was calculated within the SPT formalism. The model was able to reproduce the trends in solution behavior of C_{60} along a series of aromatic solvents. The solvation and solution properties of fullerenes C_{60} and C_{70} were compared with the model developed. The estimations of solvation properties were further extended to higher fullerenes.

Introduction

The dissolution properties of the fullerenes are still of primary importance for their manufacturing, functionalization by organic reactions and for possible applications in medicine and other areas.[1,2]

Solubility of fullerene C_{60} was measured in more than 140 solvents of different classes. The best solvents found so far are aromatics.[2,3] The best solubility (1.29×10^{-2} in molar fraction) was measured in 1-phenylnaphthalene.[4] In Table 1 the dissolution properties of C_{60} in toluene are compared with the ones of iodine in hexane. The latter solution is regular, which is typical of many organic solids. As seen from the table, the saturated solution of C_{60} in toluene is far from regularity and is characterized by a significant negative partial excess entropy of dissolution. C_{70} has the similar solution properties, though much less is known about them.[2]

Fullerenes are thought not to aggregate in aromatic solvents at equilibrium.[3,5,6]

Measured solubilities of the fullerenes are concentrations in the solutions, saturated relative to different solid phases, namely, to the solid solvates of different compositions or pristine C_{60} (C_{70}). Before observing of the trends and establishing of any correlations with solubility, it is logical to refer solubility to one and the same solid phase in every solvent, namely, to unsolvated fullerene. This was done with the knowledge of the Gibbs free energy of formation of solid solvates. The recalculated solubilities were called "hypothetical".[8,9]

Numerous attempts have been made to explain the trends in room-temperature solubility of the fullerenes.[3,9−17] Because the set of solubility data for C_{60} is large, the multiparameter statistical methods were successfully used to find correlations of solubility with the different solvent properties or parameters.[9−15] This purely statistical methodolgy is usually based on the postulated "linear solvation free energy relationships". A multiparameter artificial neural network was applied to introduce nonlinearity into the treatment.[13] It is worth noting that in refs 10−15 the statistical methodology was applied to "measured" rather than to the "hypothetical" solubilities. Though no corrections were made to the formation of solid solvates, the correlations of solubility with the solvent parameters were still found. This is typical for the purely statistical method that is not based on the solution modeling.

TABLE 1: Solution Properties of Fullerene C_{60} and Iodine I_2[a]

solute	solvent	10^3x	ΔH_{melt}, kJ·mol^{-1}	ΔH_{sol}, kJ·mol^{-1}	ΔS_{ex}, J·mol^{-}·K^{-1}
I_2[7]	*n*-hexane	5	16.7	20	0
C_{60}[2]	toluene	0.4	20[b]	−8	−101

[a] x is the solubility in molar fractions. ΔH_{melt}, ΔH_{sol}, ΔS_{ex} are enthalpy of melting, partial enthalpy of solution, and partial excess entropy of mixing of a solute, respectively, at $T = 298$ K. [b] Estimated value, based on $\Delta S_{melt} = 10$ J·mol^{-}·K^{-1}, typical for rigid spherical molecules and $T_{melt} = 2000$ K.

No thermodynamic model has been employed so far to explain fullerene solubilities. The only exceptions to mention are refs 3, 16, and 17 where the Hildenbrand solubility parameter was formally used for correlating with solubility.

In the work given the solvation free energy of a solute transfer process from the gas phase to an ideal dilute solution was represented as a sum of Gibbs free energies of cavity formation and of solute−solvent interaction. For thermodynamic description of the cavity formation in the liquid solvent the scaled particle theory (SPT) was used. Computation of the different contributions to the free energy of solute−solvent interaction was performed on the basis of the polarizable continuum model (PCM) within the standard ab initio quantum mechanical calculations by effective Hamiltonian methods.

Most theoretical approaches describing solvation phenomena allow for the direct calculation of free energy contributions. Recently, the method previously used to calculate the electrostatic free energy term within the polarizable continuum model[18] has been extended to the short-range solute−solvent dispersion and Pauli repulsion interactions computed self-consistently as a part of a solvent reaction field operator.[19]

It was expected that the balance of two contrasting factors, namely of unfavorable cavitation energy and of favorable, short-range van der Waals solute−solvent interaction energy, determines the solubility of such nonpolar molecules as fullerenes C_{60} and C_{70}. Most of the solvents do not form covalently bonded chemical compounds with C_{60} or C_{70} at room temperature. Only

10.1021/jp034567o CCC: $25.00
Published on Web 08/16/2003

slight shifts in IR, UV, or NMR spectra due to intermolecular interaction were detected. No features of charge transfer complex formation were found. Spherical molecules of the fullerenes that form monomeric diluted solutions at saturation seem to fit precisely to the basic concepts of the SPT-PCM model, described above.

Within the model we aimed to follow and to compare the trends in solubility behavior of C_{60} and C_{70} along the series of aromatic solvents.

General Outline

The solute−solvent interactions were analyzed in the framework of the continuum model with a sharp cut between the solute considered at the ab initio level and the solvent represented with a structureless polarizable medium characterized by a number of macroscopic quantities: dielectric constant, refractive index, density, etc. In this procedure the solute is embedded in a molecular-shaped cavity in the continuum solvent distribution defined in terms of interlocking spheres centered on atoms. The following general phenomenological partition for the solvation free energy was used:

$$\Delta_{solv}G = \Delta G_{cav} + \Delta G_{int} = \Delta G_{cav} + \Delta G_{el} + \Delta G_{disp} + \Delta G_{rep} + \Delta G_{ther} \quad (1)$$

where $\Delta_{solv}G$ corresponds to the free energy change for a transfer process of the solute molecule from a *fixed* position in the ideal gas phase to a *fixed* position in the solution.[20] Alternative interpretation of this value is the solvation free energy at equal numeral densities of solute in the gas phase and in the solution, e.g., 1 mol/L.[20]

In this expression, ΔG_{cav} is the Gibbs free energy of a cavity formation in the liquid solvent whereas the following three terms are the electrostatic ΔG_{el}, dispersion ΔG_{disp}, and repulsion ΔG_{rep} contributions to the free energy change ΔG_{int} due to turning on the solute−solvent interactions when the solute is in the cavity. The last term ΔG_{ther} describes the difference in rotational, vibrational, and electronic motion of the solute in the gas phase and in solution. To a first approximation, one can neglect this term. The relation between $\Delta_{solv}G$ and the measurable conventional free energy change $\Delta_{solv}G°$ is given by the expressions

$$\Delta_{solv}G° = \Delta_{sol}G° - \Delta_{sub}G° = -RT\ln x - \Delta_{sub}G° \quad (2a)$$

$$\Delta_{solv}G° = \Delta_{solv}G + RT\ln\frac{RT}{V_1°} \quad (2b)$$

where x is the fullerene molar fraction in the solution saturated in respect to the *pure solid fullerene*, $V_1°$ is the molar volume of a solvent, R is the universal gas constant, and $\Delta_{sol}G°$ and $\Delta_{sub}G°$ are standard free energies of solution and of sublimation of a solid, respectively. The standard solvation Gibbs energy $\Delta_{solv}G°$ corresponds to the following reference states: ideal gas, $P = 1$ atm and hypothetical ideal diluted solution with molar fraction of a solute equal to unity, $x = 1$.

The cavitation free energy ΔG_{cav} is expressed by applying the SPT adopted for real liquids.[21] All contributions to the interaction free energy ΔG_{int} were treated within continuum quantum mechanical methods based on effective Hamiltonians (EHCD): the fullerene−solvent interactions are accounted for by a perturbation added to the solute Hamiltonian operator for the isolated molecule. The electrostatic interaction energy ΔG_{el} was calculated using the apparent surface charge model (ASC) within the Miertus−Scrocco−Tomasi formalism.[18] Dispersion and repulsion terms ΔG_{disp} and ΔG_{rep} were calculated within the Amovilli−Mennucci approach in the polarizable continuum model (PCM)[19] by the standard SCF method. Some details of the computational procedures will be presented in the following sections.

TABLE 2: Characteristics of the Molecular Cavities of C_{60} and C_{70}

solute	V_{vdW}, Å^3	d_V, Å	S_{vdW}, Å^2	d_S, Å
C_{60}[a]	525.2	10.01	345.8	10.49
C_{70}[a]	617.8	10.57	387.6	11.11

[a] S_{vdW} is the external surface area. V_{vdW} is the sum of the molecular volume and the volume of the internal cavity of the fullerene cage; the latter amounts 5.6% of the total volume for C_{60} and 6.9% for C_{70}; r(C) = 1.70 Å.

Methods

Computational Details. The ab initio calculations were performed using the PC GAMESS version[22] of the GAMESS (US) QC package[23] at the Hartree−Fock level of theory. The computations were performed on P IV and AMD Athlon MP 1800+. Most of the empirical properties of solvents needed for calculations, such as relative permittivity ϵ, refractive index n, molar volumes $V_1°$, and ionization potential IP were extracted from the *CRC Handbook of Chemistry and Physics* and may be found in Table 8. In a few cases the NIST Chemistry WebBook data were used (http://webbook.nist.gov).

Cavitation Energy. The free energy of cavity formation term ΔG_{cav} was calculated within Reiss's and Pierotti's scaled particle theory formalism (SPT):[21]

$$\Delta G_{cav} = RT\left\{-\ln(1-y) + \frac{9}{2}\left(\frac{y}{1-y}\right)^2 r^2 + 3\frac{y}{1-y}r(1+r)\right\} + \frac{yP}{\rho_s}r^3 \quad (3)$$

where

$$y = \frac{\pi}{6}\sigma_s{}^3\rho_s \qquad r = \frac{\sigma_m}{\sigma_s}$$

The analytic expression (3) depends on, besides temperature T and pressure P, solute (cavity) diameter σ_m, effective diameter of the solvent molecule σ_s, and its numeral density ρ_s. The set of effective solvent (and also solute) molecule diameters σ_s was calculated from the corresponding van der Waal's volumes (SPT-V). The vdW volumes of solvent molecules were revealed from their equilibrium HF/6-31G(d) geometries using the standard radii data set built in the Gamess package. The set of effective solvent radii used may be found in Table 8. The geometries of the solute molecules C_{60} and C_{70} have been optimized in vacuo at the HF/6-31G(d) level of theory and were considered unchanged on solvation. The solute cavities are formed by interlocking spheres centered on atoms. The van der Waals characteristics of the corresponding molecular cavities are presented in Table 2. It should be noted that the fullerene cage contains an internal cavity that is not accessible for solvent molecules. Therefore, the volume of internal cavity enclosed was added to the excluded volume in each case, i.e., to the van der Waals volumes for C_{60} and C_{70}. The external surface area only should be considered in different continuum solvation models, e.g., for construction of the solvent accessible surface (SASA).

Electrostatic Free Energy. The favorable electrostatic contribution ΔG_{el} to the interaction free energy ΔG_{int} was

expected to be small due to the nonpolar character of solutes under consideration. The quantum mechanical calculation of this term is based on the apparent surface charge model (ASC) within the Miertus−Scrocco−Tomasi formalism.[18] The solute charge distribution is assumed to be placed in a cavity, where the relative dielectric constant is equal to unity, whereas outside, the dielectric constant has the macroscopic value ϵ of the solvent considered to be an infinite dielectric medium. The solvent reaction potential V_{el} of the polarized dielectric medium owing to the presence of the solute is described in terms of virtual charge density σ appearing on the cavity surface. For computational convenience, the charge distribution σ is discretized into induced point charges q_i located at the centers r_i of small elements into which the surface is partitioned.

$$V_{el} = \sum_i \frac{q_i}{|r - r_i|} \tag{4}$$

The electrostatic formulas giving the charges q_i using a set of linear equations expressed in the matrix form may be found elsewhere.[18,24] The induced charges depend on the normal components of the electric field on the cavity surface, dielectric constant of the solvent and geometrical cavity parameters. The electrostatic reaction potential V_{el} reduced to the field of induced point charges is then considered a perturbation to the Hamiltonian for the isolated molecule to take into account the electrostatic solute−solvent interaction in the continuum solvation model:

$$\hat{H} = \hat{H}^\circ + \hat{V}_{el} + \hat{V}_{disp} + \hat{V}_{rep} \tag{5}$$

$$\hat{H}\Psi = E\Psi \tag{6}$$

The electrostatic and also other contributions to the solvation free energy of C_{60} and C_{70} in different solvents were computed by the standard SCF method using a MINI basis set.[25] The molecular shape cavities for C_{60} and C_{70} were defined using Bondi radii, namely $r(C) = 1.70$ Å, scaled by a factor $f = 1.2$, proposed for evaluation of the electrostatic term for neutral solutes.[26] In addition, one more sphere with radius $r = 3.00$ Å was placed at the centers of both C_{60} and C_{70} molecules because internal "hollows" of the fullerene cages are not accessible for continuum solvent distribution. The effect of a small amount of solute charge distribution escaped from the cavity due to electronic tails was treated with standard renormalization procedure by applying the common correction factor for all tesserae (ICOMP = 2). It is worth noting only a slight dependence of ΔG_{el} on the type of renormalization procedure used (less than 0.5 kJ/mol) was found.

Dispersion and Repulsion Contributions. The computation of the solute−solvent dispersion interaction free energy is based on the Amovilli−Mennucci approach in the polarizable continuum model.[19] The general expression for ΔG_{disp} was obtained by exploiting the analogy between the theory of intermolecular forces between two molecules and the theory of solvation in the PCM with respect to electrostatic contribution. Details of the modelistic consideration can be found in the original papers.[19,27] The *Pauli repulsion* term ΔG_{rep} in the Amovilli−Mennucci model is proportional to the fraction of the solute electrons outside the cavity and to the average number of solvent valence electrons (n_{val}) per unit volume (V_1°):

$$\Delta G_{rep} = \alpha \frac{n_{val}}{V_1^\circ} \int_{\vec{r} \notin C} d\vec{r} P_A(\vec{r}) \tag{7}$$

TABLE 3: Dispersion Contribution to the Solvation Energy of C_{20} Dissolved in Benzene

basis set: W_1/W_2	no. of functions	ΔG_{disp}, kJ/mol	ω_A, E_h
MINI	100	−61.5	1.1793
MINI/s,p,d	300	−96.5	1.1793
MINI/2s,2p,2d	500	−136.1	1.1793
MINI/2s,2p,2d,1f	700	−145.6	1.1793

Here, P_A is the ground-state electron density of the solute and α is a constant estimated as a suitable value for the simplest two-electron system, namely He.[19] This term has the counterpart at the microscopic level as an exchange−repulsion interaction originated due to Pauli exclusion principle. The dispersion contribution ΔG_{disp} in the final expression depends on the solvent refractive index η, ionization potential IP, solute response functions in terms of ground-state electron density, and the averaged transition energy ω_A computed from the orbital energies:

$$\Delta G_{disp} = -\frac{\beta}{2} \sum_{rstu} [rs|tu] P_{ru} \left((S^{-1})_{st} - \frac{1}{2} P_{st} \right) \tag{8}$$

$$[rs|tu] = (^1/_2) \oint_{S(C)} d\vec{r} [V_{rs}(\vec{r})\, E_{tu}(\vec{r}) + V_{tu}(\vec{r})\, E_{rs}(\vec{r})] \tag{9}$$

$$\beta = \frac{\eta^2 - 1}{4\pi\eta \left(\eta + \frac{\omega_A}{IP} \right)} \tag{10}$$

Here **P** is the solute electron density matrix, **S** is the overlap matrix, V_{rs} and E_{rs} are normal components of the electrostatic potential and electric field due to the couple of basis functions χ_r, χ_s, and S(C) is the surface of molecular cavity.

It is worth mentioning that the ratio of dispersion energies calculated for one solute in different solvents was almost equal to the ratio of corresponding factors β. This surprising feature of the model could also be demonstrated with the data extracted from original papers (see Tables 2−4 in ref 19). In the present study it was used to justify the introduction of a uniform empirical scaling factor for the dispersion energies of one solute in different solvents (see below).

The test calculations proved the importance of diffuse and polarization functions in calculation of the dispersion term. For effective evaluation of ΔG_{disp} the splitting of the basis set is applied as described in the original paper.[19] The auxiliary basis functions W_2 (s,p,d) orthogonalized by a Schmidt procedure to normal basis W_1 contribute to the dispersion energy only. The W_2 basis uses exponents that are one-third of the smallest exponents in the W_1 basis. The normal basis set W_1 was employed to describe the solute electron density and contributes nearly 40% to the total ΔG_{disp} value. Table 3 demonstrates the dispersion energy ΔG_{disp} dependence on the basis dimension for the smallest fullerene molecule C_{20}. The MINI basis set was used for description of the solute wave function. The averaged transition energy ω_A was independent of the basis used, because additional basis functions W_2 changed the dispersion energy rather than the density matrix of the solute.

The application of extended basis sets W_1/W_2 for such large molecules as fullerenes C_{60} and C_{70} was problematic due to the enormous increase in the time of computations. Certain restrictions were introduced by the PCM program module (restriction on max number of functions in auxiliary basis set W_2); i.e., the approach described in ref 19 targets small and medium size solutes in the first place. To overcome this difficulty, an

TABLE 4: Gibbs Energy of Solvation for C_{60} in Different Solvents at 298 K

solvent	ΔG_{cav}, kJ·mol^{-1}	ΔG_{el}, kJ·mol^{-1}	ΔG_{rep}, kJ·mol^{-1}	ΔG_{disp}, kJ·mol^{-1}	ΔG_{tr},[a] kJ·mol^{-1}	$\Delta_{solv}G°$, kJ·mol^{-1} calc	exp
benzene[b,c]	114.0	−0.4	14.4	−263.8	13.9	−121.9	−122.0
fluorobenzene[b,c]	104.3	−0.7	16.4	−249.4	13.8	−115.7	−117.6
chlorobenzene[b,c]	117.9	−0.8	15.1	−269.0	13.6	−123.2	−123.2
bromobenzene[b,c]	126.6	−0.7	14.6	−281.1	13.5	−127.1	−126.8
iodobenzene[b,c]	137.5	−0.7	13.8	−296.5	13.4	−132.4	−131.3
toluene[b,c]	103.3	−0.4	14.5	−253.0	13.5	−122.2	−120.7
ethylbenzene[a]	100.2	−0.4	14.7	−251.9	13.1	−124.3	−120.4
anisole	123.8	−0.6	16.5	−248.0	13.4	−94.9	−122.5
1,2-dimethylbenzene	103.6	−0.5	14.9	−251.2	13.2	−120.0	−125.1
1,3-dimethylbenzene[a]	97.1	−0.4	14.6	−248.0	13.1	−123.6	−122.8
1,4-dimethylbenzene[a]	97.0	−0.4	14.6	−244.9	13.1	−120.6	−122.2
1,3,5-trimethylbenzene[a]	94.1	−0.4	14.8	−245.6	12.8	−124.3	−125.1
1,2,4-trimethylbenzene	98.1	−0.5	15.0	−244.6	12.8	−119.1	−129.0
1,2-dichlorobenzene[a]	128.0	−0.9	15.9	−280.2	13.3	−123.9	−127.6
1,3-dichlorobenzene	121.6	−0.7	15.7	−278.7	13.3	−128.8	−123.5
1,2,4-trichlorobenzene[a]	131.8	−0.9	16.5	−287.0	13.1	−126.6	−129.8
1,2-dibromobenzene[a]	145.6	−0.8	15.1	−301.9	13.2	−128.8	−131.0
1,3-dibromobenzene	135.9	−0.7	14.9	−300.0	13.2	−136.8	−131.2
1-methylnaphthalene[b,c]	118.0	−0.5	16.6	−277.3	12.8	−130.5	−130.8
1-chloronaphthalene[b,c]	126.5	−0.7	16.9	−287.0	12.9	−131.4	−131.3
water	193.8	−1.1	19.0	−232.5	17.9	−2.9	−17.4[d]
n-hexane	94.9	−0.4	12.3	−224.0	12.9	−104.1	−110.9

[a] $\Delta G_{tr} \equiv RT \ln(RT/V_1°)$. [b] Aromatic solvents presented in Figure 2a. [c] Monosubstituted benzenes and naphthalenes, presented in Figure 2b. [d] Estimated by Heymann.[17]

empirical scaling factor λ was used for evaluation of a dispersion terms ΔG_{disp}:

$$\Delta G_{disp} = \lambda \Delta G^{\varnothing}_{disp} \qquad (11)$$

where $\Delta G^{\varnothing}_{disp}$ is the dispersion energy calculated using restricted (minimal) basis sets.

The value of this empirical scaling factor was thought to be the same for all solvents studied due to the fact that the dispersion term is expanded into two factors (see eq 8), only one of which depends on the empirical solvent properties, namely, the refractive index and ionization potential. The application of the identical extended basis sets has to scale dispersion contributions *uniformly* for all the solvents.

The solute wave function and unscaled $\Delta G^{\varnothing}_{disp}$ values were treated using the MINI atomic basis set for both C_{60} and C_{70}. The following averaged transition energies for the fullerenes were obtained: $\omega_A(C_{60}) = 1.295$ hartree and $\omega_A(C_{70}) = 1.274$ hartree. The value of scaling factor λ in eq 11 for C_{60} fullerene was found by the least-squares method within the comparison of calculated (eq 1) and experimental (eq 2) solvation free energies

$$\Delta_{solv}G(\text{exp}) = \lambda \Delta G^{\varnothing}_{disp} + \Delta G_{cav} + \Delta G_{rep} + \Delta G_{el} \qquad (12)$$

in 18 aromatic solvents. This procedure gave $\lambda = 2.427 \pm 0.025$. The three last terms in the right-hand side of the eq 12 are independent of specific extension of the atomic basis chosen. Then, we adopted the same scaling factor λ and the same formula (8) for computation of ΔG_{disp} values for C_{70}. It is worth noting that the optimized value of λ for C_{60} is rather close to the ratio of ΔG_{disp} obtained for C_{20} with MINI/2s,2p,2d,1f and MINI basis sets, respectively (2.367; see Table 1).

Results and Discussion

Thermodynamics of Solvation of C_{60} and C_{70}. The results of calculation of the total Gibbs free energies of solvation and their contributions are presented in Tables 4 and 5. The solvents include 20 aromatic compounds, water, and *n*-hexane. Experimental solvation free energies are based on "hypothetical" solubilities of C_{60} and C_{70}[2,8,9] and sublimation free energies ($T = 298$ K): $\Delta_{sub}G°(C_{60}) = 140$ kJ/mol and $\Delta_{sub}G°(C_{70}) = 155$ kJ/mol.[28] The sum of the numbers in columns 2−4 (Tables 4 and 5) gave $\Delta_{solv}G$ (see eq 1) whereas "calculated" (column 6) and "experimental" (column 7) $\Delta_{solv}G°$ were calculated by eqs 1, 2b, and 2a, respectively.

As can be seen from Tables 4 and 5, the favorable electrostatic contribution ΔG_{el} to the interaction free energy ΔG_{int} is negligible, in comparison with others; the absolute value of this term increasing with dielelectric constant of a solvent. Analysis of the calculated ΔG_{el} values enables us to construct the following analytic approximation:

$$\Delta G_{el} = -\delta(1 - \epsilon^{-\gamma})$$

where

$$\gamma = 0.5-0.6 \qquad \delta > 0$$

The main contributions to the solvation free energy are the positive (unfavorable) cavitation free energy and negative (favorable) dispersion interaction free energy; the absolute value of ΔG_{disp} being 2.0−2.5 times larger than ΔG_{cav}. The dispersion interaction energy in this model goes up with increasing of both refractive index η and ionization potential IP of a solvent. ΔG_{rep} contributes near 12% to the total solvation energy. This term is proportional to the average number of solvent valence electrons per volume unit. The calculations showed that the free energy of cavity formation ΔG_{cav} correlates *linearly* with interaction free energy contribution ΔG_{int} for *aromatic solvents:* $\Delta G_{int} = -1.184\Delta G_{cav} - 117.6$, $R^2 = 0.98$ (see Figure 1). Probably, this reflects the universal character of interaction among *solvent* molecules in pure liquids and *solute−solvent* interactions: the increased intermolecular interactions in the pure solvent could lead to increased *favorable* solute−solvent dispersion interactions.

TABLE 5: Gibbs Energy of Solvation for C_{70} in Different Solvents at 298 K

solvent	ΔG_{cav}, kJ·mol^{-1}	ΔG_{el}, kJ·mol^{-1}	ΔG_{rep}, kJ·mol^{-1}	ΔG_{disp}, kJ·mol^{-1}	ΔG_{tr},[a] kJ·mol^{-1}	$\Delta_{solv}G°$, kJ·mol^{-1} calc	exp
benzene	125.8	−0.4	15.9	−301.5	13.9	−146.3	
fluorobenzene	115.0	−0.8	18.2	−285.1	13.8	−138.9	
chlorobenzene	130.1	−0.8	16.8	−307.5	13.6	−147.9	
bromobenzene	139.7	−0.8	16.2	−321.3	13.5	−152.6	
iodobenzene	151.8	−0.8	15.3	−338.8	13.4	−159.1	
toluene	113.9	−0.5	16.1	−289.1	13.5	−146.2	−137.1
ethylbenzene	110.5	−0.5	16.3	−287.9	13.1	−148.6	
anisole	136.6	−0.7	18.3	−283.5	13.4	−116.0	
1,2-dimethylbenzene	114.3	−0.5	16.5	−287.1	13.2	−143.7	−144.2
1,3-dimethylbenzene	107.0	−0.5	16.2	−283.4	13.1	−147.6	
1,4-dimethylbenzene	106.9	−0.5	16.2	−279.9	13.1	−144.3	−138.3
1,3,5-trimethylbenzene	103.7	−0.5	16.4	−280.8	12.8	−148.4	−144.2
1,2,4-trimethylbenzene	108.4	−0.5	16.6	−279.6	12.8	−142.3	
1,2-dichlorobenzene	141.2	−1.0	17.7	−320.2	13.3	−149.0	−147.5
1,3-dichlorobenzene	134.2	−0.8	17.5	−318.5	13.3	−154.4	−140.2
1,2,4-trichlorobenzene	145.4	−1.0	18.3	−328.0	13.1	−152.2	
1,2-dibromobenzene	160.8	−0.9	16.8	−345.0	13.2	−155.2	
1,3-dibromobenzene	150.0	−0.8	16.5	−342.8	13.2	−164.0	
1-methylnaphthalene	130.1	−0.6	18.4	−317.0	12.8	−156.3	
1-chloronaphthalene	139.5	−0.8	18.8	−328.0	12.9	−157.6	
water	214.5	−1.2	21.1	−265.6	17.9	−13.4	
n-hexane	104.6	−0.4	13.7	−255.9	12.9	−125.1	

[a] $\Delta G_{tr} \equiv RT \ln(RT/V_1°)$.

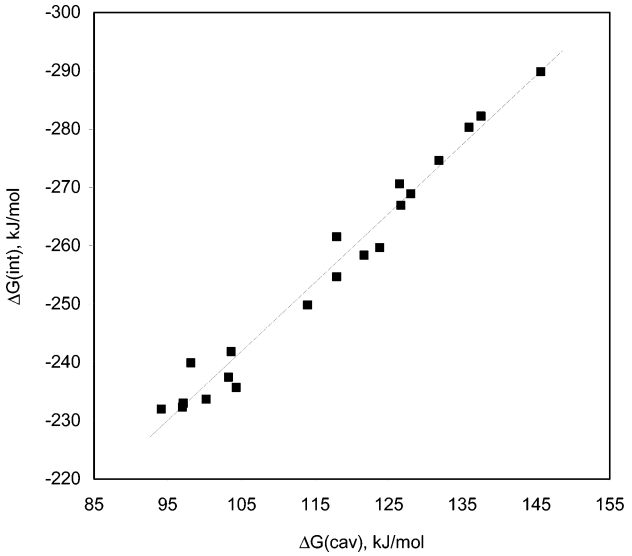

Figure 1. Correlation of the cavitation and interaction free energies for C_{60} solvated by 20 different aromatic solvents.

The model reproduces the *experimental* trends across the family of 15 aromatic solvents in Table 4. The mean error with respect to the experimental solvation free energies is 1.42 kJ/mol, rms error 1.92 kJ/mol (see Figure 2a). The outliers not included in the correlation in Figure 2a are anisole and 1,2,4-trimethylbenzene, 1,2-dimethylbenzene, 1,3-dichlorobenzene, 1,3-dibromobenzene (the errors for the last four solvents are above twice the average absolute difference between experimental and calculated solvation free energy data for 19 aromatic solvents (excluding anisole), i.e., $\Delta_i > 5$ kJ/mol).

The model also qualitatively accounts for the change of solvation properties of C_{60} on going from aromatic solvents to hexane and water.

However, solution behavior in *positional* isomers of disubstituted benzenes was not predicted correctly. The solubility of C_{60} is higher in 1,2-disubstituted benzenes compared to 1,3-derivatives although the solubilities in 1,2- and 1,3-dibromobenznes are practically equal. The PCM calculations made the ΔG_{int} values 1.5−3 kJ/mol more negative for 1,2-isomers in comparison with 1,3-isomers due to the slightly larger refractive index of the formers, but less positive ΔG_{cav} values were obtained for 1,3-derivatives compared to 1,2-derivatives because the latter have slightly higher densities.

In Figure 2b the SPT-PCM correlation is compared with one of the results, obtained with the statistical methodology.[9] The quality of the SPT-PCM fit in this particular case is better (mean error is 0.64 kJ/mol compared to 2.99 kJ/mol with data of ref 9).

The extremely low solubility of C_{60} in water is explained by ΔG_{cav}, which is much more positive than in aromatic solvents. The dispersion free energy of C_{60} in water is also less favorable. Solubility of C_{60} in *n*-hexane is lower compared to aromatic solvents. The main reason is the significant decrease of the dispersion free energy. ΔG_{disp} is lower for C_{60} in hexane due to the lower polarizability (lower refraction index η in eq 8, 10) of *n*-hexane in comparison with the aromatic solvents.

Comparison of Solution Properties of C_{60} and C_{70}. The C_{70} molecule is larger than C_{60} by 10 additional carbon atoms. The free energies of cavity formation ΔG_{cav} in the *same* solvents are more positive for C_{70} than the ones for C_{60}. There is a linear correlation between these two sets of values, namely

$$\Delta G_{cav}(C_{70}\text{ in S}) = 1.103\Delta G_{cav}(C_{60}\text{ in S}) \qquad R^2 = 0.999$$

for 20 aromatic solvents.

The slope of this correlation is close to the ratio of external molecular surface areas of $S_{vdW}(C_{70})$ to $S_{vdW}(C_{60})$, equal to 1.121. On the other hand, the favorable interaction free energies are more negative for C_{70} in comparison with C_{60} because the former solute is larger (e.g., in terms of the solvent-accessible surface). In case of universal van der Waals type interactions, this term usually increases with the size of the solute because the number of atoms and electrons increase. PCM calculations show that

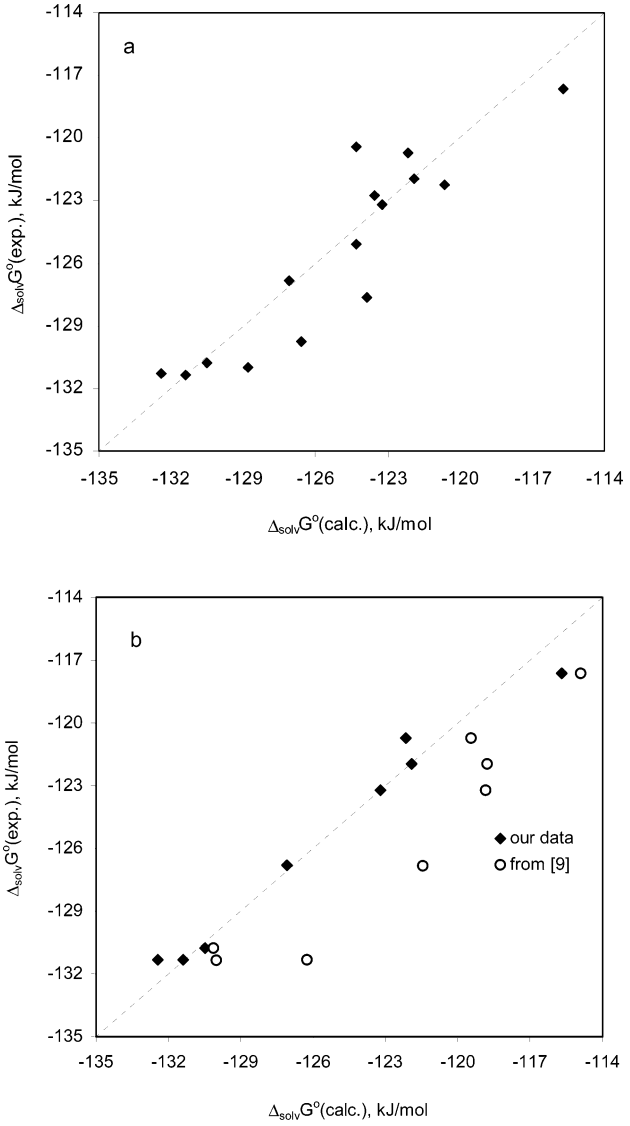

Figure 2. Correlation of the calculated vs experimental solvation free energies of C_{60} in different solvents: (a) C_{60} solvated by 15 different aromatic solvents (see Table 4); (b) C_{60} solvated by 8 monosubstituted benzenes and naphthalenes. Key: (◆) calculated data from the present study (see Table 4); (○) calculated data from ref 9.

there is a strong correlation between ΔG_{int} values for C_{60} and C_{70} solvated by the *same* solvents:

$$\Delta G_{int}(C_{70}\text{ in S}) = 1.145\Delta G_{int}\,(C_{60}\text{ in S}) \qquad R^2 = 0.999$$

for 20 aromatic solvents.

The slope of the correlation is slightly more than the external molecular surface area ratio.

Table 6 presents *experimental* (column 9) and *calculated* (column 8) *solution* free energies $\Delta_{sol}G^{\circ}$ of C_{60} and C_{70} along with different calculated contributions to *calculated* $\Delta_{sol}G^{\circ}$ of C_{60} and C_{70} (columns 2−7) in all six aromatic solvents, where solution free energies $\Delta_{sol}G^{\circ}$ were experimentally determined for both C_{60} and C_{70}. In all six cases the experimentally determined *hypothetical* solubility of C_{70} exceeds those of C_{60}.

According to the model developed, C_{70} is *more soluble* than C_{60} in aromatic solvents because *favorable* changes in free energies of *interaction* of solute with solvent, when going from C_{60} to C_{70} (−35 kJ/mol), overcome the *unfavorable* changes in the *cavitation* energies (+11 kJ/mol) and thermodynamic stability of the solids in terms of $\Delta_{sub}G^{\circ}$ (+15 kJ/mol) (see Table 6).

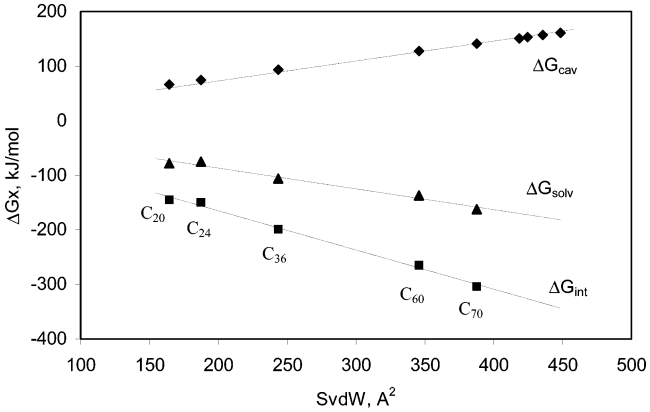

Figure 3. Gibbs free energies $\Delta G_{cav}(C_{20}-C_{84})$, $\Delta G_{int}(C_{20}-C_{70})$, and $\Delta G_{solv}(C_{20}-C_{70})$ for the series of fullerenes in *o*-dichlorobenzene vs the external molecular surface areas S_{vdW} of the fullerene cages.

TABLE 6: Comparison of Solution Free Energies of C_{60} and C_{70} in Solvents S[a]

solvent/ fullerene	ΔG_{el}, kJ·mol^{-1}	ΔG_{rep}, kJ·mol^{-1}	ΔG_{disp}, kJ·mol^{-1}	ΔG_{cav}, kJ·mol^{-1}	ΔG_{int}, kJ·mol^{-1}	$\Delta_{sol}G^{\circ}$, kJ·mol^{-1} calc	exp
toluene							
C_{60}	−0.4	14.5	−253.0	103.3	−238.9	17.9	19.3
C_{70}	−0.5	16.1	−289.1	113.9	−273.5	8.8	17.9
o-xylene							
C_{60}	−0.5	14.9	−251.2	103.6	−236.8	20.0	15.0
C_{70}	−0.6	16.5	−287.1	114.3	−271.1	11.3	10.8
p-xylene							
C_{60}	−0.4	14.6	−244.9	97.0	−230.7	19.4	17.8
C_{70}	−0.5	16.2	−279.9	106.9	−264.3	10.7	16.7
mesitylene							
C_{60}	−0.4	14.8	−245.6	94.1	−231.3	15.7	14.9
C_{70}	−0.5	16.4	−280.8	103.7	−264.9	6.6	10.8
o-$C_6H_4Cl_2$							
C_{60}	−0.9	15.9	−280.2	128.0	−265.2	16.1	12.4
C_{70}	−1.0	17.7	−320.2	141.2	−303.5	6.0	7.5
m-$C_6H_4Cl_2$							
C_{60}	−0.7	15.7	−278.7	121.6	−263.7	11.3	16.5
C_{70}	−0.8	17.5	−318.5	134.2	−301.9	0.6	14.8

[a] $\Delta_{sub}G^{\circ}(C_{60}) = 140$ kJ/mol and $\Delta_{sub}G^{\circ}(C_{70}) = 155$ kJ/mol at $T = 298$ K.[28]

The model predicts also the strong correlation of the *solution* free energies of C_{60} and C_{70} in different solvents:

$$\Delta_{sol}G^{\circ}(C_{70}\text{ in S}) = 1.159\Delta_{sol}G^{\circ}(C_{60}\text{ in S}) - 12.252 \qquad R^2 = 0.997$$

where

$$\Delta_{sol}G^{\circ} = -RT\ln x = \Delta_{solv}G^{\circ} + \Delta_{sub}G^{\circ}$$

Thus, C_{70} is more soluble in "good", e.g., aromatic, solvents but less soluble in the "bad" solvents such as water with large positive free energy of cavity creation. The transition in solution behavior may be predicted as $\Delta_{sol}G^{\circ}(C_{60}) = +77$ kJ/mol, corresponding to the negligible fullerene solubility $\approx 10^{-14}$ in the molar fraction scale.

The correlations found may be extended to the higher fullerenes. Figure 3 demonstrates almost excellent correlation of ΔG_{cav} , ΔG_{int}, and $\Delta_{solv}G$ for the series of fullerenes in *o*-dichlorobenzene with the external molecular surface areas S_{vdW} of the fullerene cages.

TABLE 7: Solvation Gibbs Free Energies of Fullerenes in *o*-Dichlorobenzene at 298 K

fullerene	ΔG_{cav}, kJ/mol	ΔG_{int}, kJ/mol	S_{vdW}, Å	$\Delta_{solv}G$, kJ/mol
C_{20} (I_h)	66.5	−144.6	164.4	−78.1
C_{24} (D_6)	74.6	−149.6	187.4	−75.0
C_{36} (D_{6h})	93.4	−199.2	243.4	−105.9
C_{60} (I_h)	128.0	−265.2	345.8	−137.2
C_{70} (D_{5h})	141.2	−303.5	387.6	−162.3
C_{76} (D_2)	150.9	*−322.3*[a]	418.7	*−170.3*[a]
C_{78} (C_{2v})	153.0	*−326.5*	424.6	*−172.5*
C_{80} (D_2)	156.9	*−334.4*	435.6	*−176.8*
C_{84} (D_{2d})	161.2	*−343.8*	448.6	*−181.7*

[a] In italic: values estimated through linear correlation with external molecular surface areas S_{vdW}.

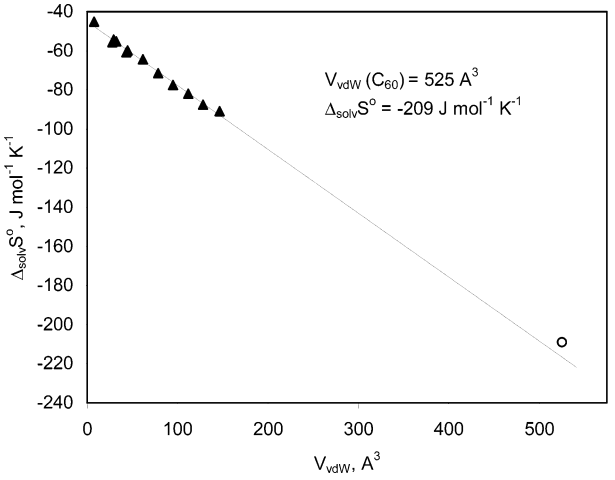

Figure 4. Correlation of the *experimental* entropies of solvation of different solutes (inert gases, *n*-alkanes) and C_{60} in benzene vs vdW volumes of the solutes.

ΔG_{cav} and S_{vdW} were calculated for the series of existing fullerenes (see Table 7). For the first five cages in Table 7 (C_{20}−C_{70}) ΔG_{int} and the resulting ΔG_{solv} were calculated using the MINI basis and eq 8. For the rest of the fullerenes (C_{76}−C_{84}) the Gibbs free energies of interaction and solvation were estimated through the linear correlation with the S_{vdW} (see Table 7).

The competition of two factors (unfavorable increase of ΔG_{cav} and favorable decrease in ΔG_{int}) leads to the monotonic decrease of $\Delta_{solv}G$ (better solvation!) for higher fullerenes in aromatic solvents (see Figure 3). The solubility (or $\Delta_{sol}G°$) of the higher fullerenes in turn will also depend on the stability of the corresponding crystal lattices, i.e., on $\Delta_{sub}G°$ (see eq 2). There is no reason to expect simple dependence of the latter value on the size of the carbon cluster. It is known that a family of higher fullerenes with small HOMO−LUMO gaps, such as C_{74}, etc., form very stable insoluble solids.[29]

Entropies of Solvation. With the model described above, an attempt was made to reproduce the remarkable solvation entropies of the fullerenes in aromatic solvents. The SPT formula for ΔG_{cav} enables one to calculate the entropy of cavity formation by differentiation of ΔG_{cav} with respect to temperature. Dependence of ΔS_{cav} on the cavity radius in most of organic solvents goes through a minimum, changes the sign, and becomes positive at the certain critical diameter of a cavity depending on the solvent properties. It means that in accordance with SPT we have positive ΔS_{cav} values for such large solutes as fullerenes in such solvents as benzene, toluene, carbon tetrachloride, *n*-hexane, etc. The usual additional assumption is that only cavity creation is accompanied by an entropy loss and solvent reorganization whereas the solute−solvent attractive interactions in the first approximation do not influence the solvent structure and therefore contribute to the enthalpy of solvation rather than to the entropy and solvent reorganization energy, i.e., $\Delta G_{int} \approx \Delta H_{int}$ and $\Delta S_{int} \approx 0$.[21,26] For fullerenes C_{60} and C_{70} the SPT entropies of cavity formation were compared with the "experimental" entropies ΔS_{cav} calculated from the experimental ΔG_{solv} and ΔH_{solv}[2,8] under the assumption $\Delta S_{int} \approx 0$. It was demonstrated that the correlation between the experimental and the calculated numbers does not exist. For C_{60} in toluene the "experimental" ΔS_{cav} is equal to −171 $J \cdot K^{-1} \cdot mol^{-1}$ whereas SPT-based values vary from 2 to 33 $J \cdot K^{-1} \cdot mol^{-1}$ depending on the effective solvent diameters adopted (σ_s = 5.64−5.74 Å). For C_{70} in toluene the corresponding numbers are −222 and +4−38 $J \cdot K^{-1} \cdot mol^{-1}$, respectively. SPT calculations complemented with the $\Delta S_{int} \approx 0$ guess always yield entropies of solvation ΔS_{solv} that are much less negative in comparison with the observed ones for large and middle size solutes and go up with an increase in solute size, whereas the experimental ΔS_{solv} values always go down (become more negative) with the size increase.[30] The reasons for this

TABLE 8: Solvent Properties Used

solvent	formula	*M*, g/mol	V_m, cm^3/mol	σ_s, Å	ϵ	*n*	IP, eV	n_{val}
benzene	C_6H_6	78.11	89.12	5.410	2.28	1.5011	9.25	30
fluorobenzene	C_6H_5F	96.10	93.99	5.470	5.47	1.4684	9.20	36
chlorobenzene	C_6H_5Cl	112.56	101.79	5.728	5.69	1.5241	9.06	36
bromobenzene	C_6H_5Br	157.01	105.02	5.842	5.45	1.5597	8.98	36
iodobenzene	C_6H_5I	204.01	111.43	6.027	4.59	1.6200	8.69	36
toluene	C_7H_8	92.14	106.29	5.742	2.38	1.4961	8.82	36
ethylbenzene	C_8H_{10}	106.17	122.46	6.057	2.45	1.4959	8.77	42
anisole	C_7H_8O	108.14	108.79	5.910	4.30	1.5174	8.21	42
1,2-dimethylbenzene	C_8H_{10}	106.17	120.62	6.043	2.56	1.5055	8.56	42
1,3-dimethylbenzene	C_8H_{10}	106.17	122.85	6.043	2.36	1.4972	8.56	42
1,4-dimethylbenzene	C_8H_{10}	106.17	123.30	6.051	2.27	1.4958	8.44	42
1,3,5-trimethylbenzene	C_9H_{12}	120.19	138.92	6.326	2.28	1.4994	8.41	48
1,2,4-trimethylbenzene	C_9H_{12}	120.19	137.23	6.266	2.38	1.5048	8.27	48
1,2-dichlorobenzene	$C_6H_4Cl_2$	147.00	112.57	6.010	10.12	1.5515	9.08	42
1,3-dichlorobenzene	$C_6H_4Cl_2$	147.00	114.10	6.011	5.02	1.5459	9.11	42
1,2-dibromobenzene	$C_6H_4Br_2$	235.91	118.89	6.213	7.86	1.6155	8.98	42
1,3-dibromobenzene	$C_6H_4Br_2$	235.91	120.84	6.214	4.81	1.6083	9.01	42
1,2,4-trichlorobenzene	$C_6H_4Cl_3$	181.45	124.37	6.266	-	1.5717	9.04	48
1-methylnaphthalene	$C_{11}H_{10}$	142.20	139.38	6.483	2.92	1.6170	7.96	54
1-chloronaphthalene	C_9H_7Cl	162.62	136.22	6.467	5.04	1.6326	8.13	54
water	H_2O	18.02	18.07	2.995	78.4	1.3252	12.61	8
n-hexane	C_6H_{14}	86.18	131.61	6.196	1.89	1.3749	10.13	38

discrepancy may arise both from inadequacy of highly simplified solvent model used in SPT and from possible inadequacy of the assumption $\Delta S_{int} \approx 0$. The results of a number of recent papers,[31,32] however, made us to think that the former factor rather than the latter is significant. The Monte Carlo simulations of different alkanes (normal, branched, and cyclic) and also their associated molecular shape cavities solvated by water, including the enthalpy and entropy changes in addition to the solvation free energies showed that the process of turning on the attractive van der Waals interactions rescales the solute−solvent potential energy but has a small effect on the solvent reorganization.[31] The entropies of hydration of these solutes were found to be mainly determined by the entropy of their associated cavities whereas turning on the solute−solvent attractive van der Waals and electrostatic interactions is accompanied by small entropy changes. This observation is also valid when the size of the molecular system grows although the interaction free energies increase. At the same time it was found that the enthalpy−entropy decomposition of the SPT free energy of cavity formation ΔG_{cav} based on the experimental thermal expansion coefficient of organic liquids α_P is in contradiction with results obtained by MD simulations.[33] Thermodynamics of cavity formation in *n*-hexane was studied in ref 33 using the Widom particle insertion method. The entropy change was found to be considerably more negative compared to SPT. It decreased monotonically with the radius of a cavity whereas SPT predictions lead to the opposite conclusion. Nevertheless, the $\Delta G_{cav}(r)$ values calculated within SPT formalism for different spherical cavities of radius *r* are in reasonable agreement with the results of Monte Carlo and MD simulations of the cavity insertion process, at least for water and *n*-hexane.[33,34] One may conlude that SPT enables one to model the *free energy* of cavity creation rather than its temperature-dependent *entropy* and *enthalpy* contributions.

The main part of the negative entropy gain in the solvation process may be explained by the "excluded" volume effect. The solvent excluded volume created by the solute is responsible for the entropy loss due to the reduced number of solvent configurations in the solution in comparison with bulk solvent (translational entropy loss).[31,35] The more negative entropy of solvation of C_{70} in comparison with C_{60} may be explained by increasing of the solvent "excluded" volume on going from C_{60} to C_{70}. The decrease of the solvation entropies in organic liquids and water with the growing size of a neutral solute is a general tendency. Figure 4 presents ΔS_{solv} vs van der Waals volume dependence for different solutes (alkenes, inert gases) in benzene.[30] The linear trend gives for C_{60} the entropy change $\Delta_{solv}S°$ equal to -216 J·K^{-1}·mol^{-1}, in good agreement with the experimental value (-209 J·K^{-1}·mol^{-1}).

Conclusions

In the present study we attempted to describe the solvation and the solution of fullerenes using the SPT-PCM formalism. According to the SPT-PCM model the solvation behavior of the fullerenes is determined mainly by the competition of the favorable dispersion interaction energy (ΔG_{disp}) and the unfavorable energy of the cavity formation (ΔG_{cav}). Our calculations showed that the free energy of cavity formation ΔG_{cav} correlates *linearly* with the interaction free energy contribution ΔG_{int} for aromatic solvents. Based on the solvation free energies it was possible to predict correctly the general trends in solubility of C_{60} along the series of aromatic solvents and the transition to hexane and water. Prediction of the more specific trends such as better solubility in ortho isomers compared to meta isomers of benzene derivatives was not possible because only "rough" bulk properties are used to characterize the solvent in SPT-PCM. Comparison of solubilities of C_{60} and C_{70} based on the SPT-PCM solvation energies was also performed because the difference in Gibbs free energies of sublimation for two fullerenes is known from the literature. The better solubility of C_{70} in aromatic solvents was explained by the favorable increase in ΔG_{disp} only, because other factors work in the opposite direction. Simple correlation of the interaction Gibbs free energy with geometrical parameters of the fullerene cages was used also for the higher fullerenes. This is a promising way of predicting the solvation, but not the solubility properties, of the higher fullerenes, because the very different stability of the higher fullerene solids will definitely change the regular trends predicted by SPT-PCM for solvation Gibbs free energies of the higher fullerenes.

The entropy of solvation of C_{60} correlates with the large vdW volume of the solute. The large negative partial entropies of solvation of the fullerenes may be explained by the "solvent excluded volume effect".

Acknowledgment. The work was supported by RFBR (grants 00-03-32097 and 03-03-32186).

References and Notes

(1) Da Ros, T.; Prato, M. *Chem. Commun*. **1999**, 663−669.
(2) Korobov, M. V.; Smith, A. Solubility of the fullerenes. In *Fullerenes*; Kadish, K., Ruoff, R., Eds.; John Wiely & Sons Inc: New York, 2000; pp 53−91.
(3) Beck, M. T.; Mandi, G. *Fullerene Sci. Technol.* **1997**, *5*, 291−310.
(4) Ruoff, R. S.; Tse, D. S.; Malhotra, R.; Lorents, D. C. *J. Phys. Chem.* **1993**, *97*, 3379−3383.
(5) Catalan, J.; Saiz, J. L.; Laynez, J. L.; Jagerovic, N.; Elguero, J. *Angew. Chem., Int. Ed. Engl.* **1995**, *34*, 105−107.
(6) Honeychuck, R. V.; Cruger, T. W.; Milliken, J. *J. Am. Chem. Soc.* **1993**, *115*, 3034−3035.
(7) Hildenbrand, J.; Scott R. *Regular Solutions*; Prentice Hall: Englewood Cliffs, NJ, 1962.
(8) Korobov, M.; Mirakian, A.; Avramenko, N.; Ollofson, G.; Ruoff, R.; Smith, A. L. *J. Phys. Chem. B* **1999**, *103*, 1339−1346.
(9) Marcus, Y.; Smith, A.; Korobov, M.; Mirakyan, A.; Avramenko, N. A.; Stukalin, E. B. *J. Phys. Chem. B* **2001**, *105*, 2499−2506.
(10) Murray, J. S.; Gagarin, S. G.; Poltzer, P. *J. Phys. Chem*. **1995**, *99*, 12081−12083.
(11) Smith A. L.; Wilson L. Y.; Famini G. R. A Quantitative Structure−Property Relationship Study of C_{60} Solubility. In *Recent Advances in the Chemistry and Physics of Fullerenes and Related Materials*; Ruoff, R. S., Kadish, K. D., Eds.; The Electrochemical Society Inc.: NJ, 1996.
(12) Danauskas, S.; Jurs, P. *J. Chem. Inf. Comput. Sci*. **2001**, *41*, 419−424.
(13) Kiss, I.; Mandi, G.; Beck, M. *J. Phys. Chem. A* **2000**, *104*, 8081−8088.
(14) Marcus, Y. *J. Phys. Chem.* **1997**, *101*, 8617−8623.
(15) Abraham, M.; Green, C.; Acree, W. *J. Chem. Soc., Perkin Trans.* **2000**, *2*, 281−286.
(16) Sivaraman, N.; Dhamodaran, B.; Kaliappan, I.; Srinivasan, T. G.; Vasudeva Rao, P. R.; Mathews, C. K. *J. Org. Chem.* **1992**, *57*, 6077−6079.
(17) Heymann D. *Carbon* **1996**, *34*, 627−631.
(18) Miertus, S.; Scrocco, E.; Tomasi, J. *Chem. Phys.* **1981**, *55*, 117−129.
(19) Amovilli, C.; Menuccii, B. *J. Phys. Chem. B* **1997**, *101*, 1051−1057.
(20) Ben-Naim, A. *J. Phys. Chem*. **1978**, *82*, 792−803.
(21) Pierotti, P. *Chem. Rev*. **1976**, *76*, 717−726.
(22) Granovsky, A. A. www http://classic.chem.msu.su/gran/gamess/index.html.
(23) Schmidt, M. W.; Baldridge, K. K.; Boatz, J. A.; Elbert, S. T.; Gordon, M. S.; Jensen, J. J.; Koseki, S.; Matsunaga, N.; Nguyen, K. A.; Su, S.; Windus, T. L.; Dupuis, M.; Montgomery, J. A. *J. Comput. Chem.* **1993,** *14*, 1347−1363.
(24) Miertus, S.; Tomasi, J. *J. Chem. Phys*. **1982,** *65*, 239.
(25) Tatewaki, H.; Huzinaga, S. *J. Comput. Chem.* **1980**, *1*, 205−216.
(26) Tomasi, J.; Persico, M. *Chem. Rev.* **1994**, *94*, 2027−2094.
(27) Amovilli, C. *Chem. Phys. Lett.* **1994**, *229*, 244−249.

(28) CRC Handbook of Chemistry and Physics, 77th ed.; CRC Press: Boca Raton, FL, 1996.
(29) Diener, M.; Alford, J. *Nature* **1998**, *393*, 668−671.
(30) Abraham, M. H.; Nasehzadeh, A. *J. Chem. Soc., Faraday Trans.* **1981,** *1*, *77*, 321−340.
(31) Gallicchio, E.; Kubo, M. M.; Levy, R. M. *J. Phys. Chem. B* **2000**, *104*, 6271−6285.
(32) Kubo, M. M.; Gallicchio, E.; Levy, R. Manuscript in preparation.
(33) Tomas-Oliveira, I.; Wodak, S. J. *J. Chem. Phys.* **1999,** *111*, 8576−8587.
(34) Floris, F. M.; Selmi, M.; Tani, A.; Tomasi J. *J. Chem. Phys.* **1997,** *107*, 6353−6365.
(35) Ashbaugh, H.; Paulaitis M. *J. Phys. Chem.* **1996**, *100*, 1900−1913.